Molecular Vision 2017; 23:963-976 <http://www.molvis.org/molvis/v23/963>
Received 17 April 2017 | Accepted 15 December 2017 | Published 17 December 2017

Oligodendrocyte death, neuroinflammation, and the effects of minocycline in a rodent model of nonarteritic anterior ischemic optic neuropathy (rNAION)

Zara Mehrabian,[1] Yan Guo,[1] Daniel Weinreich,[3] Steven L. Bernstein[1,2]

[1]Department of Ophthalmology, University of Maryland School of Medicine, Baltimore, MD; [2]Department of Anatomy and Neurobiology, University of Maryland School of Medicine, Baltimore, MD; [3]Department of Pharmacology, University of Maryland School of Medicine, Baltimore, MD

Purpose: Optic nerve (ON) damage following nonarteritic anterior ischemic optic neuropathy (NAION) and its models is associated with neurodegenerative inflammation. Minocycline is a tetracycline derivative antibiotic believed to exert a neuroprotective effect by selective alteration and activation of the neuroinflammatory response. We evaluated minocycline's post-induction ability to modify early and late post-ischemic inflammatory responses and its retinal ganglion cell (RGC)–neuroprotective ability.

Methods: We used the rodent NAION (rNAION) model in male Sprague-Dawley rats. Animals received either vehicle or minocycline (33 mg/kg) daily intraperitoneally for 28 days. Early (3 days) ON-cytokine responses were evaluated, and oligodendrocyte death was temporally evaluated using terminal deoxynucleotidyl transferase dUTP nick end labeling (TUNEL) analysis. Cellular inflammation was evaluated with immunohistochemistry, and RGC preservation was compared with stereology of Brn3a-positive cells in flat mounted retinas.

Results: Post-rNAION, oligodendrocytes exhibit a delayed pattern of apoptosis extending over a month, with extrinsic monocyte infiltration occurring only in the primary rNAION lesion and progressive distal microglial activation. Post-induction minocycline failed to improve retinal ganglion cell survival compared with the vehicle treated (893.14 vs. 920.72; $p>0.9$). Cytokine analysis of the rNAION lesion 3 days post-induction revealed that minocycline exert general inflammatory suppression without selective upregulation of cytokines associated with the proposed alternative or neuroprotective M2 inflammatory pathway.

Conclusions: The pattern of cytokine release, extended temporal window of oligodendrocyte death, and progressive microglial activation suggests that selective neuroimmunomodulation, rather than general inflammatory suppression, may be required for effective repair strategies in ischemic optic neuropathies.

Nonarteritic anterior ischemic optic neuropathy (NAION) is the most common cause of sudden optic nerve–related vision loss, affecting about 6,000 individuals in the United States each year [1]. Although the etiology of NAIONs is still debated, the lesion is based on a sudden or rapidly progressive ischemic insult to the anterior optic nerve (ON), resulting in capillary and retinal ganglion cell (RGC)–axonal dysfunction, followed by astrocyte activation, oligodendrocyte distress and death, and inflammation [1]. Following disruption of the blood–brain barrier in rodents and primates, an acellular inflammation gives way to extrinsic inflammatory cell invasion, microglial activation, and migration into the primary ischemic lesion [2,3]. Although the timing of RGC loss and retinal gene activation has been investigated [4,5], the timing of the ON inflammatory response, oligodendrocyte death, and multiple effects of inflammation on repair and recovery are poorly understood. Oligodendrocyte death occurs after either traumatic or ischemic ON damage, along with axonal loss [6], but the timing of oligodendrocyte loss has not been directly evaluated.

Since the ON is a central nervous system (CNS) white matter tract, its inflammatory response post-injury likely resembles that of other white matter tracts [2,6,7]. Following the CNS ischemic insult, the upregulation and release of cytokines include TNF-α, IL-1β, IL-6, -10, and G-CSF, and chemokines including MCP-1 and CX3CL1 (Fractalkine) [8]. One day after induction of rodent NAION (rNAION), the ischemic optic nerve upregulates mRNAs for TNF-α, IL-1β, IL-6, and MIP-2/CXCL2 [9,10]. The specific release of cytokines or chemokines can direct the succeeding cellular inflammatory response [11]. Although neurodegenerative inflammation (the M1 classical response) typically predominates, evidence has mounted that an alternative inflammatory response (the M2 response) may exist that predisposes to neurorepair. Until recently, CNS microglial responses were believed to model the M1/M2 pathways identified in extrinsic macrophage

Correspondence to: S.L. Bernstein, Lab of Molecular Research, Department of Ophthalmology, University of Maryland at Baltimore, Baltimore, MD 21201; Phone: (410) 706-4482; FAX: (410) 706-7057; email: sbernstein@som.umaryland.edu

responses [12]. However, new reports, suggest that the M1/M2 hypothesis for microglia is inaccurate [13,14]. This does not eliminate the overall approach of immunomodulatory therapies directed to reduce post-ischemic damage. Rather, it is germane to understand the overall effects of modulating the immune response to develop effective treatments for optic nerve and other CNS ischemic conditions.

Minocycline is a tetracycline derivative that can exert neuroprotective effects in models of hypoxia and ischemia in the CNS and reduce white matter damage [15,16]. Minocycline's reported effects seem to be related to inflammatory modulation, including inhibiting microglial responsiveness [17], reducing neurodegenerative microglial responses [18], and inhibiting production of proinflammatory cytokines and microglia-associated neurotoxicity [19]. Microglia-mediated neurodegeneration is associated with oxidative stress [20,21]. However, several reports suggested that minocycline administration is associated with decreased oxidative stress [22]. Minocycline was recently reported to exert some degree of neuroprotection in models of glaucoma and traumatic optic neuropathy [23-25]. In all latter studies, minocycline was given before the initiation of retinal stress. Because little predictability exists regarding the exact timing of clinical NAION onset, even in individuals with multiple risk factors, NAION pretreatment is by and large impractical. Thus, we wanted to determine the following: 1) the timing of oligodendrocyte death following induction of the rNAION model, 2) whether minocycline treatment is retinal ganglion cell (RGC)–neuroprotective following rNAION induction, 3) the effect of minocycline-related alterations, if any, in superoxide radical formation in the ON following rNAION induction, and 4) the effect of minocycline on cytokine protein expression post-rNAION at the 3 day time point, when alterations in the inflammatory cellular infiltrate may direct effective neuroprotection.

METHODS

All animal protocols were approved by the institutional IACUC and adhered to the ARVO Statement for Use of Animals in Research. Male Sprague-Dawley outbred rats (200–300 g; 55–75 days old) from Harlan, Indianapolis, IN were used in this study. rNAION was induced as previously described [4]. Animals were anesthetized with ketamine/xylazine (50 mg/2 mg/kg) anesthesia. A 7 mm custom planoconvex contact lens was used to stabilize the eye and visualize the rat fundus. rNAION was photoinduced after intravenous rose bengal dye injection (2.5 mM; 1 ml/kg) using a frequency doubled 532 nm YAG laser (Iridex; 11 s/50 mW/500 µm spot). Retina fundi were evaluated with fundus photography using a digital camera and with spectral domain-optical coherence tomography (SD-OCT; Heidelberg Instruments, Heidelberg, Germany) at baseline and 2 days post-induction for ON damage after stroke, visualizing the retinal cell layers and the ON diameter using the previously described planoconvex contact lens. Animals were returned to their cages and given food and water ad libitum on a 12 h:12 h light-dark cycle.

In vivo imaging:: The optic nerve head edema was evaluated using SD-OCT, via a Heidelberg Spectralis II (Heidelberg Instruments). The retina and the intraocular portion of the ON were visualized through the dilated pupil using a planoconcave contact lens that enabled analysis of the retinal layers [26].

Animals were euthanized at specific times with intracardiac perfusion with 4% paraformaldehyde-PBS (PFA-PBS) pH 7.4 , PBS formulation (1X;120 mM NaCl, 20 mM KCl, 10 mM $NaPO_4$, 5 mM KPO_4, pH 7.4). Ocular tissues were isolated, and tissues post-fixed for 1 day in 4% PFA-PBS. Tissues were cryopreserved in 30% sucrose, embedded in optimal cutting temperature compound (OCT), and sectioned at 10 µM.

Animal experimental groups:

ON apoptosis—Thirty-three animals were used for this experiment: Nine animals were unilaterally induced for the 31 day time point, with three animals used for all other times. The fellow eye was used as a control (naïve). Animals were euthanized at 1, 3, 7, 10, 15, 21, 31, 36, and 42 days post-induction. We performed terminal deoxynucleotidyl transferase dUTP nick end labeling (TUNEL) analysis using cross sections from ON specimens 5 mm distal to the eye, except at the 31 day time point, when we assayed distal and anterior ON regions (1–2 mm behind the eye). The TUNEL assay used a commercially available fluorescent tag kit (Roche Life Sciences; Indianapolis, IN) according to the manufacturer's protocol. Appropriate positive control and negative control sections were included. We included data from anterior and distal ON regions. We confirmed cellular apoptosis of oligodendrocytes using immunohistochemistry, via colocalization of rabbit anti-adenoma polyposis-1 (APC1) protein (RRID: AB_91789; Calbiochem, La Jolla, CA) and cleaved goat anti-caspase-3 (RRID: AB_630987; Santa Cruz Biotechnology, ,Dallas, TX) staining. Sections were visualized with an E900 fluorescent digital confocal microscope (Olympus, Tokyo, Japan).

Minocycline-RGC neuroprotection analysis: Data were collected from rNAION-induced animals: 17 eyes

(minocycline) and 15 eyes (vehicle). Minocycline-treated animals received 33 mg/kg minocycline hydrochloride (Sigma, St. Louis, MO). Naïve controls were the untreated contralateral eyes from the vehicle-treated animals. Animals received daily intraperitoneal injections for 4 weeks. Control animals received a similar volume of sterile saline. Eyes were collected, and retinal cups reacted with goat anti-Brn3a antibody (RRID: AB_630987; Santa Cruz Biotechnology), with secondary Cy3-labeled anti-goat antibody. Retinas were flat mounted for stereological analysis.

Early and late inflammation histochemical analysis: Data were collected from animals at 3, 7, and 30 days post-induction, from anterior and distal ON regions. Other CNS tissues were not evaluated. An additional five animals per group were used at 30 days for the MitoSOX Red (Molecular Probes, Life Technologies, Eugene, OR; free radical assay) experiments. Tissues were reacted with antibodies for specific for global inflammation. They included rabbit Iba1 (RRID: AB_839504; Wako Chemicals USA, Inc., Richmond, VA); NADPH oxidase-subunit 2 (Nox2; RRID: AB_11016938), ED1 (CD68; RRID: AB_1141557), and intact axonal neurofilaments were evaluated using an SMI 312 mouse monoclonal antibody cocktail (RRID: AB_448151) all from Abcam (Cambridge, MA). Gliosis was evaluated using an antibody to GFAP (RRID: AB_10013382) from DAKO Cytomation (Glostrup, Denmark) and demyelination using an antibody to myelin basic protein (MBP; RRID: AB_1841021; Sigma). Oligodendrocyte progenitor cells (OPCs) were evaluated with NG2 antibody (RRID: AB_91789; EMD Millipore, Billerica, MA) immunostaining.

Cytokine protein analysis: Rodent NAION was unilaterally induced in ten animals. Five rats were injected daily intraperitoneally with minocycline, while five control group animals received saline. Animals were euthanized without perfusion 3 days post-rNAION induction, and the optic nerve lamina and anterior 2 mm of the ON behind the globe was collected and pooled for each group. Tissue was sonicated on ice in lysis buffer, containing a 2 mM EDTA, protease, and phosphatase inhibitor cocktail (Cell Signaling, Danvers, MA). Tissue homogenates were centrifuged at 10,000 ×*g* for 30 s to remove debris. Cleared homogenates were analyzed using the Milliplex RECYTMAG-65K (EMD Millipore) rat Cytokine/Chemokine Luminex panel, which is based on paramagnetic beads internally dyed with fluorophores of differing intensities. Each dyed bead is given a unique number, or bead region, allowing the differentiation of one bead from another. Individual bead sets are then coated with a capture antibody qualified for one specific cytokine and combined in a 96-well microplate format assay to detect and quantify multiple targets (panel) simultaneously, using a Luminex® instrument for analysis. We followed the manufacturer's protocol in sample preparation; Luminex analysis was performed at the UMAB core facility.

RGC stereology: Retinal ganglion cell loss was evaluated using Stereo Investigator software (MBF Bioscience, Waltham, MA). Unbiased RGC stereology was performed on flat mounted whole retinas 30 days post-induction, using the optical fractionator technique, on a Nikon E800 microscope, Melville, NY with a motor-driven stage driven by the stereological software to generate random fields of up to seven cell nuclei for counting, using a 60X oil objective, and 20 µM depth in the Z-axis. A minimum of 1,000 Brn3a-positive cells were counted per retina, which is greater than the number required by the Schmitz-Hof equation for statistical validity [27].

TEM ultrastructure: PF-PBS fixed ON specimens were further processed in a mixed buffered glutaraldehyde-paraformaldehyde solution, shadowed with uranyl acetate, embedded in Epon, and cross-sectioned at 200 nm thickness. Cross sections were floated on copper mesh and examined using a Tecnai FEI T12 electron microscope (FEI, Hillsboro, OR). Images were analyzed at 2,100X magnification.

MitoSOX Red assay for superoxide radicals: We used 12 animals (two groups; n = 6/group) for this analysis. Thirty days after induction of rNAION, the ONs of the minocycline- and saline-treated Sprague-Dawley rats were dissected into 2–3 mm pieces and immersed in a 5 µM solution of MitoSOX Red (Molecular Probes, Life Technologies) for 30 min at 37 °C in darkness. Tissue was subsequently rinsed twice and fixed in 4% PFA, 10 mm sections were cut and fixed on slides, and MitoSOX Red fluorescence was monitored at about 510/580 nm. All data were compared to the results from the naïve ONs.

Compound action potentials: ON compound action potentials (CAPs) were performed as described in detail [28]. We used three animals per group. The rat ON contains three discernible classes of myelinated fibers based upon distinct populations of CAP conduction velocities [28]. Conduction velocities were estimated by measuring the length of the ON (the distance between the orifice of the stimulating and recording suction electrodes) and dividing this value by the time interval between the end of the shock artifact and the individual peaks of the CAPs.

RESULTS

The intact rodent ON has bundles of SMI 312–positive axons surrounded by MBP-positive myelin sheaths (Figure 1A). The signals for both markers are evenly distributed in the naïve ON (Figure 1A). SMI 312–positive axons are completely surrounded by MBP-positive myelin (Figure 1A, arrowheads). In contrast, ONs from 30 days post-rNAION induction reveal severe loss of signal (Figure 1B), with a non-uniform loss of axonal neurofilaments and myelin (Figure 1B inset). At higher magnification (Figure 1B), demyelination is evident, and myelin immunoreactivity is poorly associated with a non-uniform neurofilament signal, suggesting loss of intact axons and demyelination. This is better delineated with transmission electron microscopy (TEM; Figure 1C,D). TEM cross sections of intact rodent ON reveal nearly all large and small axons are intact with regular myelination (Figure 1C, arrows). Thirty days post-induction, there is considerable axonal loss, and many remaining axons are dysmyelinated (Figure 1D, arrows).

GFAP is expressed during reactive gliosis [29]. We identified reactive astrocytic and GFAP expression by reacting control and rNAION-induced ON with dilute (1:20,000) GFAP

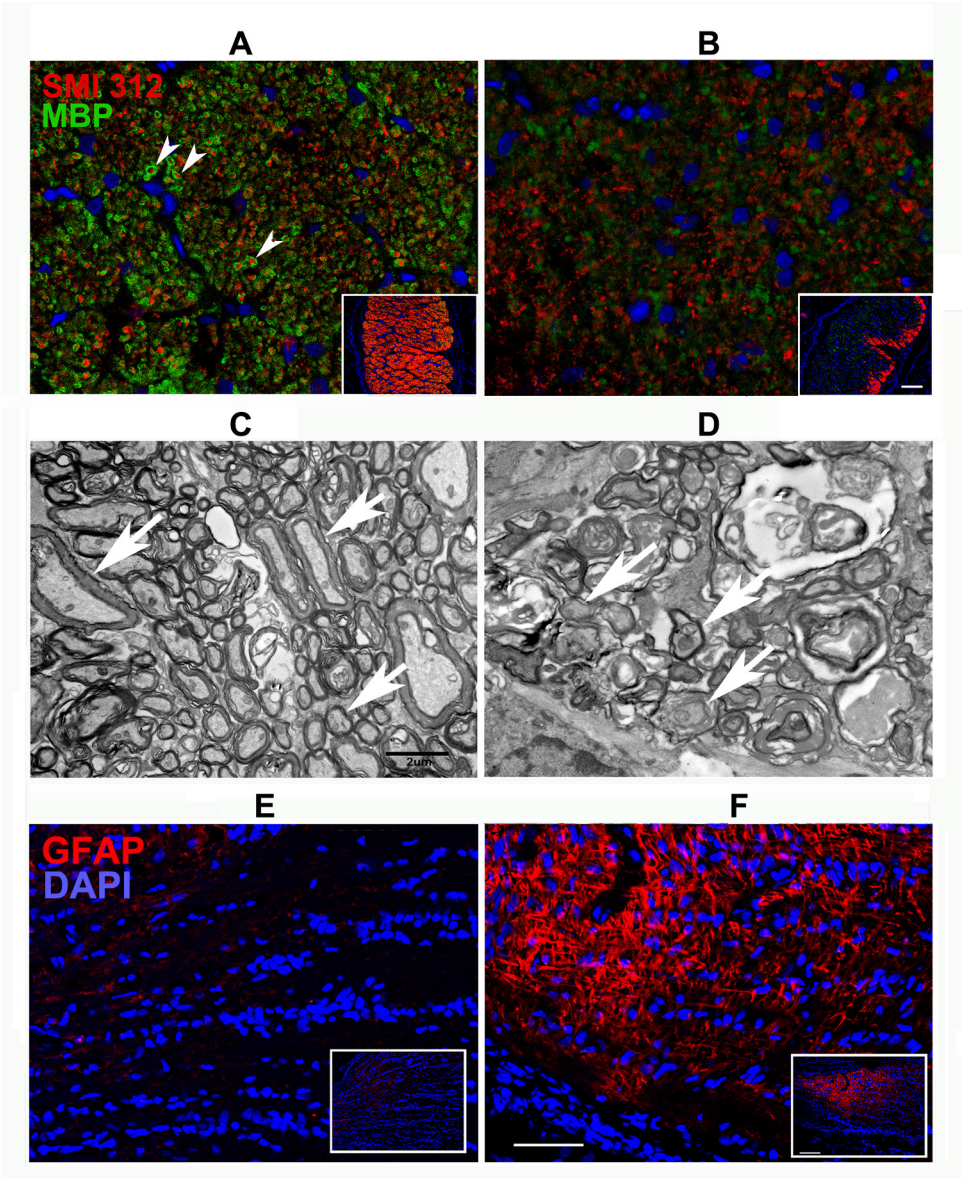

Figure 1. Analysis of axonal neurofilaments and myelination in control and rNAION-induced (30 days post-induction) ON. **A**,**B**: SMI 312 (neurofilament) and MBP (myelin) immunostaining in the control rat optic nerve (ON; **A**) and 30 days post-induction (**B**). SMI 312 immunoreactivity is seen in red. MBP is shown in green. Arrowheads indicate complete myelination (in green) of individual axons. The axonal dropout and loss of normal myelin signal and structure are typical for optic nerves following ON ischemia (**B** inset). Scale bar (inset: 100 µm). **C**,**D**: Transmission electron microscope (TEM) imaging of tissues seen in **A** and **B**. **C**: Control ON. TEM reveals normally myelinated axons of various calibers (arrows indicate relative ratios of myelination in large, medium and small axons). **D**: Rodent nonarteritic anterior ischemic optic neuropathy (rNAION)-induced ON. In contrast to the control ON, there are myelin loss, hypomyelination, and poorly compacted myelin (arrows) in the remaining axons 30 days after induction. Magnification = 2,100X. Scale bar: 2 µM. **E**,**F**: ON ischemia-induced gliosis in the anterior ON. **E**: Control ON. Anti-GFAP antibody (1:20,000 dilution) shows minimal staining in normal tissue (scale bar = 50 µm). Inset shows low magnification (scale bar: 200 µm). **F**: Post-rNAION. Strong GFAP signal is present in the anterior ON region 30 days post-induction, reflecting upregulation of astrocyte-based reactive gliosis.

antibody (Figure 1E,F). We chose this antibody dilution to identify relative changes in GFAP expression compared to total GFAP expression, because higher antibody concentrations can mask differences in upregulation. We confirmed the adequacy of this assay for reactive gliosis-associated GFAP signal, using the rat brain subjected to traumatic brain injury (TBI) compared to sham injury. The TBI brain sections yielded about sixfold greater GFAP signal than those of sham regions with densitometry. Control ONs show reduced GFAP staining (Figure 1E and inset), while the rNAION-induced ONs reveal strong GFAP immunoreactivity in an irregular, nonlinear pattern (Figure 1F and inset).

rNAION results in delayed oligodendrocyte death: Minimal oligodendrocyte death occurs early after rNAION induction, despite strong upregulation of stress-related (cfos) gene expression by 3 days [30]. In the ON crush and rNAION models, oligodendrocyte loss occurs by apoptosis [31]. Apoptosis was most notable in the anterior portion of the ON. We evaluated the timing of the appearance of TUNEL-positive nuclei in the ON from 0 to 42 days post-induction (Figure 2C), comparing the results to those previously obtained for RGC loss in the same model and rodent species [5]. Unlike RGCs, oligodendrocyte death was minimal during the first week (5.2±1.1 at 7 days; Figure 2C), with most TUNEL-positive cells presenting considerably later following injury. The majority of TUNEL-positive nuclear expression occurred between 21 and 36 days (Figure 2C; also see Figure 2B,C, TUNEL activity at 31 days and the graph), with the maximum number of TUNEL-positive nuclei present at 31 days post-induction (45.6±9.60; Figure 2C). Thereafter, oligodendrocyte loss dropped markedly, reaching exhibiting levels similar to that seen in the first week by 42 days (4.2±1.9; Figure 2C). An overlay of the previously reported temporal pattern of rNAION-associated RGC death is also shown in Figure 2C for comparison (dotted line) [5]. RGC apoptosis peaks at about 10–12 days, with a second minor peak at day 21. Thus, the majority of oligodendrocyte death begins after most RGC death has ended. Apoptosis and microglial activation were discernable throughout the entire length of the ON, but activity for both was greatest in the anterior ON. For apoptosis, the number of TUNEL-positive cells was statistically significantly higher (113.25±9.6000 standard error of the mean [SEM], n = 9) in the anterior ON compared to the more distal portion (45.60±13.02 SEM, n = 9; ANOVA f-ratio = 17.08519, p=0.003283; Figure 2D). Asterisks indicate statistical significance. This was confirmed with cleaved caspase-3 immunostaining.

The TUNEL staining conditions make it problematic to identify cell-specific proteins with immunohistochemistry. Therefore, we confirmed oligodendrocyte identity and death using a known oligodendrocyte cellular marker, antibody to adenoma polyposis coli (APC) [32] and colocalizing with cleaved caspase 3 (Figure 2E,F). Cleaved caspase activity in APC-positive cells 30 days after rNAION was quantified via densitometry using Image J. The ratio of cleaved caspase to APC was 6.9-fold higher in ONs 30 days post-rNAION versus naïve controls (0.36±0.05 SEM for naïve versus 2.49±0.06 SEM, n = 3 ONs/group, ANOVA; f-ratio = 1294.64021, p<0.00001). The absolute identification of all cell types undergoing apoptosis in the ON was considered beyond the scope of this study.

Following anterior ON ischemia, there is disruption of the blood–brain barrier [10], extrinsic inflammatory cell invasion, microglial activation, and migration into the primary ON ischemic lesion and distally. This is shown in Figure 3A–D. The strong ED1 expression at 30 days (Figure 3C,D) probably represents chronic microglial inflammation [33], rather than continuing invasion of extrinsic macrophages.

Minocycline has been suggested to exert neuroprotection via inhibition of inflammation, oxidative stress, and apoptosis, as well as inhibiting microglial activation. We compared minocycline's effects with vehicle on inflammation-associated ON damage and axonal loss post-rNAION, using immunostained optic nerve cross sections of rats from minocycline- and saline-treated groups, using inflammatory (Iba1) and axonal markers (SMI 312; Figure 4A–C,E,F and calculations for Iba1 expression, Figure 4J). Post-rNAION induction, we compared ON edema from minocycline- and vehicle-treated animals via SD-OCT against those obtained preinduction (Figure 4D). ON edema was present 2 days post-rNAION induction in all induced eyes, compared with the naïve eye (Figure 4D, compare upper and lower panels). There were no differences seen in the degree of edema between vehicle- and minocycline-treated eyes (data not shown).

Microglia in uninduced ON have a ramified appearance (Figure 4A), which changes upon inflammatory activation [34]. Three days post-induction, ON microglia from vehicle-treated animals developed an activated, hypertrophic appearance (Figure 4B). Microglia in ON sections from a similar region from rNAION-induced, minocycline-treated animals although increased in number expressed a morphological characteristic more typically associated with resting microglia, namely, a ramified structure at 3 days post-induction (Figure 4C). This was demonstrable even 30 days post-induction in minocycline-treated animals (Figure 4F) compared with vehicle-treated animals (Figure 4E,J). We further evaluated functional changes associated with these

morphological modifications (see cytokine figures and Nox2 (Figure 4G–I,K) results).

To determine whether minocycline potentially preserves axons, we compared relative axonal preservation from 30 days post-induction in vehicle- and minocycline-treated animals using SMI 312 immunohistochemistry (Figure 4E,F insets; compare with Figure 4A inset, naïve). Both groups had a qualitatively similar degree of axonal loss. Minocycline did not preserve intact RGC axons at 30 days (Figure 4E,F), and the SMI 312 signal in whole nerves showed similar degrees of dropout (compare insets, Figure 4E,F).

We also evaluated Iba-1 cell signal strength, using densitometric analysis via Image J in 30 days post-induction animals (Figure 4J). Although the data show statistically a significantly increased Iba-1 signal when compared between naïve and vehicle-treated animals (1.50±0.15 SEM vs. 7.08±0.54 SEM, six animals per group; asterisks indicate statistical significance), as well between naïve and minocycline-treated (6.72±0.97 SEM, six animals per group) animals, the difference in Iba-1 staining when comparing vehicle- versus minocycline-treated animals was not statistically significant (ANOVA; f-ratio = 0.11571, p=0.74154; Figure 4J). Morphologically, the microglia from the minocycline-treated animals were more ramified but larger compared with the activated microglia seen in the vehicle-treated animals, which had a more ameboid appearance.

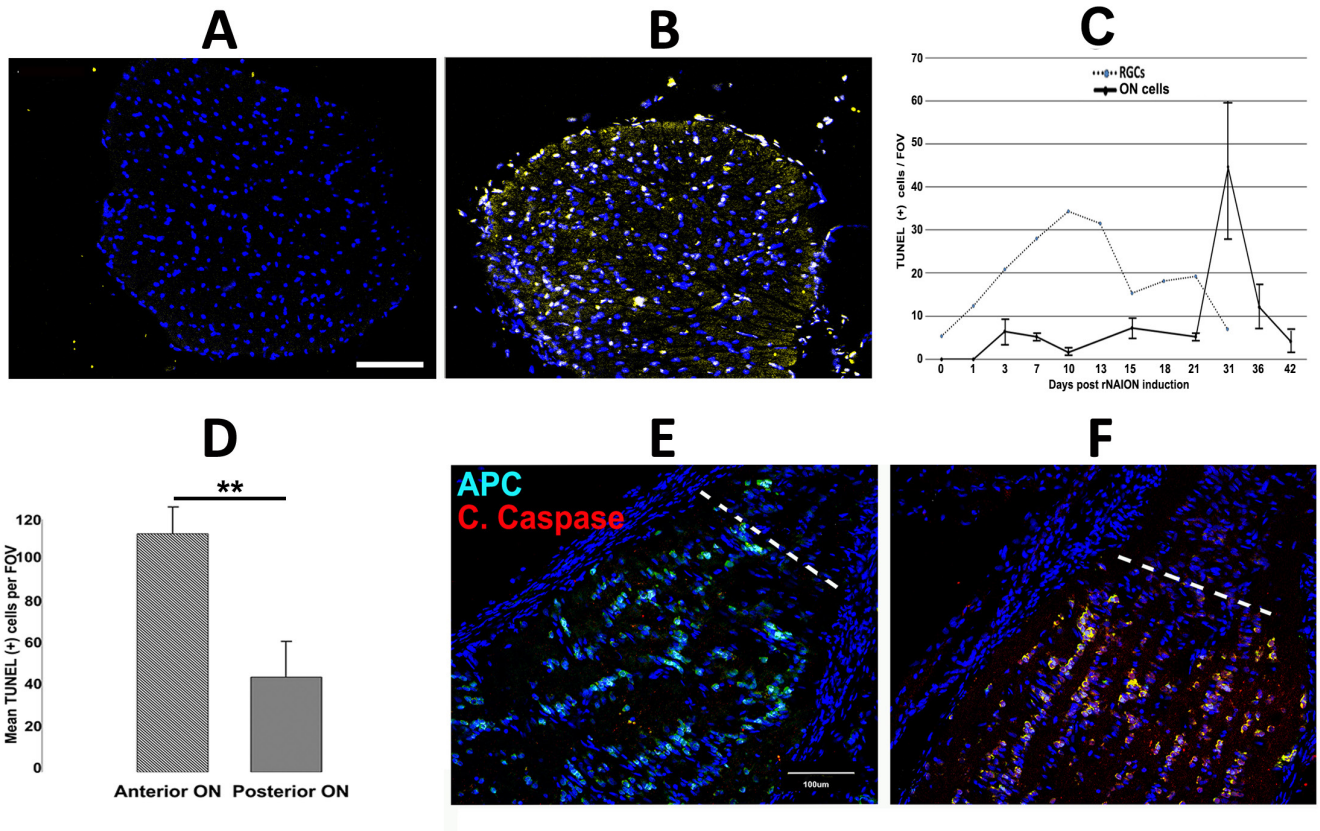

Figure 2. Cell death analysis of ON-associated apoptosis following rNAION. Optic nerve (ON) cross sections were evaluated with the terminal deoxynucleotidyl transferase dUTP nick end labeling (TUNEL) reaction in (**A**) the control (naïve) animals and (**B**) in animals 31 days after the induction of rodent nonarteritic anterior ischemic optic neuropathy (rNAION). **C**: Temporal analysis of TUNEL-positive ON cells following rNAION. Retinal ganglion cell (RGC) death timing post-rNAION (taken from [5]) is superimposed. **D**: TUNEL analysis was greatest in the anterior ON (113.25±9.6000 standard error of the mean (SEM), n = 9) compared to the more distal portion (45.60±13.02 SEM, n=9). Asterisks indicate statistical significance (ANOVA f-ratio = 17.08519, p=0.003283). **E**, **F**: Confocal analysis of APC (oligodendrocyte marker) and a marker of apoptosis (cleaved caspase 3: **C**: Caspase) in longitudinal ON sections of the anterior ON (dotted line depicts the lamina). **E**: Control (naïve). There is minimal cleaved caspase 3 expression in the anterior ON. **F**: 30 days post-rNAION. There is extensive colocalization of cleaved caspase 3 and APC in the anterior ON, suggesting the oligodendrocytes are undergoing apoptosis. The ratio of cleaved caspase to APC was 6.9-fold higher in ONs 30 day post-rNAION versus naïve controls (0.36±0.05 SEM for naïve versus 2.49±0.06 SEM, n=3 ONs/group; ANOVA; f-ratio-1294.64021, p<0.00001).

NADPH oxidase subunit-2 (Nox2; Gphos91 subunit) upregulation is associated with increased oxidative radical formation and was identified as a necessary step for glial cell activation following CNS damage [33]. We evaluated the ability of chronic minocycline administration to downregulate ON-Nox2 30 days post-rNAION induction (Figure 4G–I).

Minimal Nox2 expression is present in the naïve anterior rodent ON (Figure 4G). However, dramatic upregulation of Nox2 occurs 30 days post-NAION induction in vehicle-treated animals (Figure 4H). In comparison, minocycline treatment statistically significantly reduced Nox2 upregulation (Figure 4I). This was confirmed using densitometric analysis, comparing naïve (white bar) 11.5±1.20 SEM, vehicle-treated (black bar) 17.07±1.500 SEM, and minocycline-treated animals (hatched bar) 10.06±0.610 SEM, which was statistically significant between the naïve and vehicle-treated animals (asterisks) but not between the naïve and minocycline-treated animals (ANOVA; f-ratio = 10.51066; p=0.014213; Figure 4K). We also confirmed post-rNAION upregulation of free radicals and their downregulation by minocycline using the MitoSOX Red reaction. There was statistically significantly more MitoSOX Red signal in the vehicle-treated nerve (black bar) 87.60±20.34 SEM, compared with minocycline (Figure 4L, hatched bar) 27.0±19.9 SEM. (ANOVA; f-ratio = 9.05275; p=0.023738); the asterisk indicates statistical significance. The vehicle and minocycline numbers were greater than that seen in the naïve nerve (white bar), 5.6±3.4.

Neural/glial antigen-2 (NG2; also known as chondroitin sulfate proteoglycan-4 (CSPG4)) positive OPCs are known to increase after chronic CNS injury [35]. We analyzed NG2 expression in naïve and 30 days post-induced ONs (Figure 5A; naïve and Figure 5B; rNAION-induced). Quantification of NG2-positive cells in the two groups is shown in Figure 5C. We found substantially increased (7.1-fold) numbers of NG2-positive cells in the anterior ON region following rNAION (28.7±2.70 v. 4.0±1.9 SEM cells/field of view (FOV; n = 6 animals; Figure 5C, asterisks indicate statistical significance, ANOVA; f-ratio = 55.09054, p = 0.000023).

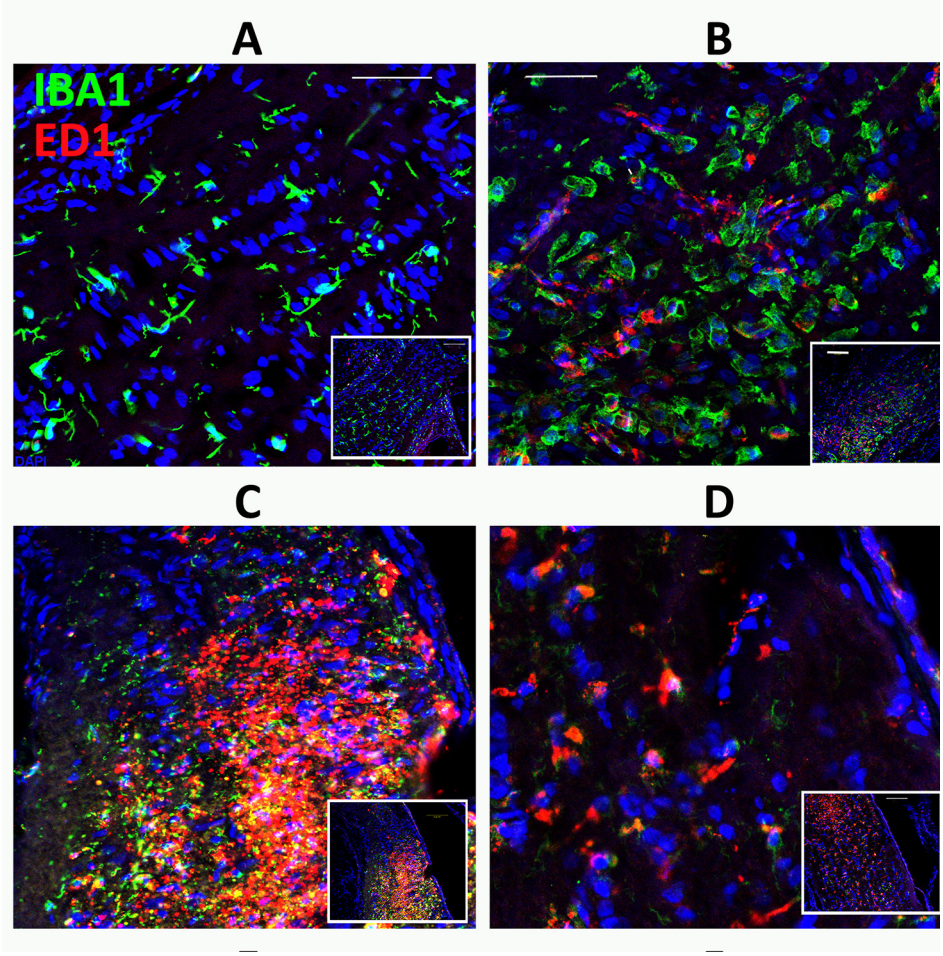

Figure 3. Inflammatory cells acquire a hypertrophic morphology and newly synthesized microglia increases in the ON following rNAION. Iba1 (Green) is a global inflammatory marker. ED1 (red) represents newly generated macrophages/microglia. **A**: Control (naïve) optic nerve (ON). Quiescent resident microglia are demonstrable as Iba1(+)/ED1(-) ramified structures (scale bar: 50 µm). Insets show images at lower magnification (200 µm). **B**: Anterior ON 3 day post-rodent nonarteritic anterior ischemic optic neuropathy (rNAION). The majority of Iba1-positive cells are now globoid (activated macrophages), and ED1-positive colocalization is present, indicating newly synthesized macrophages. **C**: Anterior ON section 30 days post-rNAION. There is strong Iba1/ED1-positive colocalization, and the anterior region is packed with inflammatory cells. **D**: Distal ON section 30 days post-rNAION.

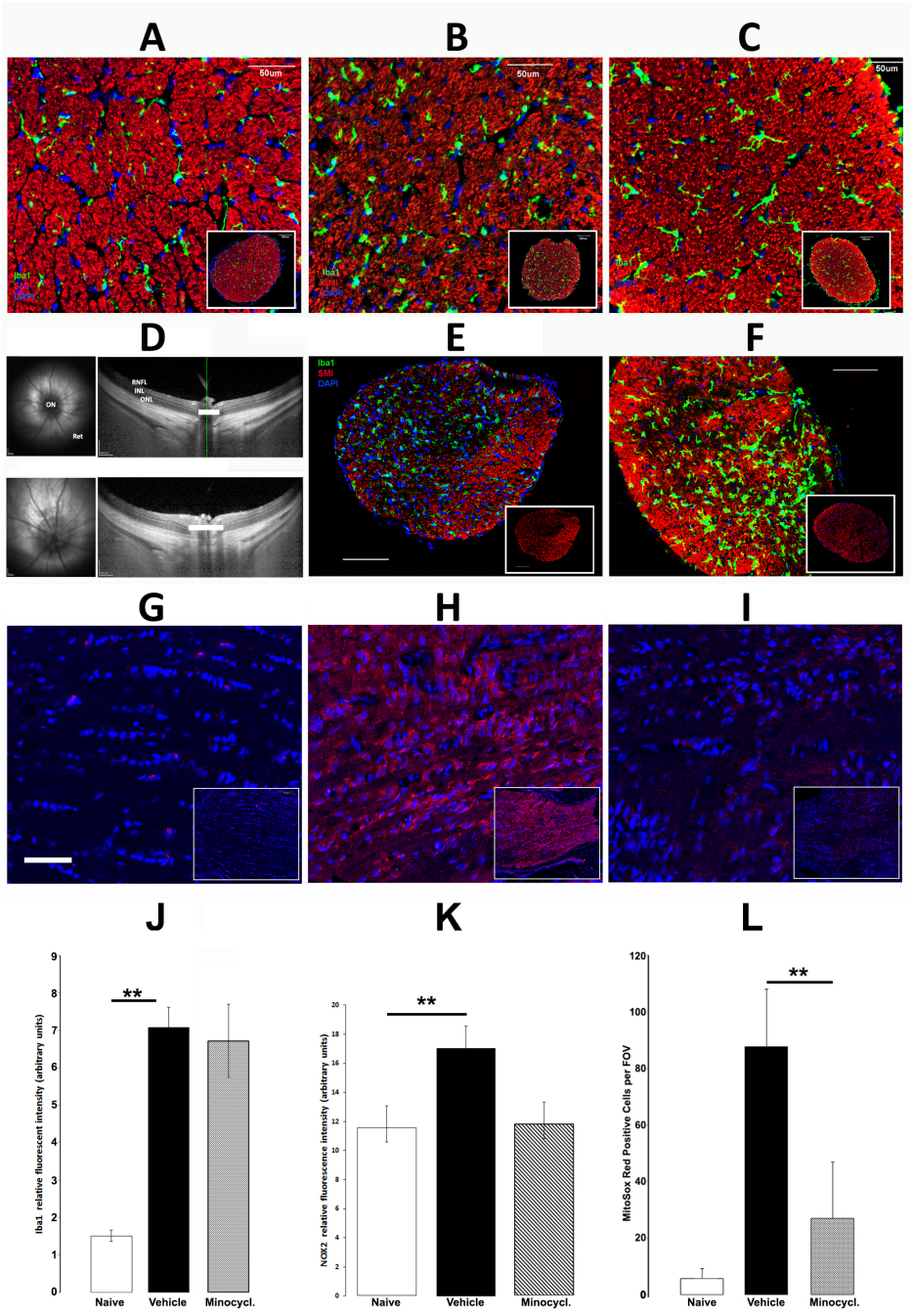

Figure 4. Minocycline-associated changes in post-ischemic ON responses. **A**–**C** and **E**,**F**: Microglial (Iba1) and axonal (SMI 312) immunohistochemistry in the optic nerve (ON; Iba1: green; SMI 312: red). **A**: Naïve ON. Microglia are evenly distributed and ramified in appearance. SMI 312–positive axons are organized into bundles. **B**: Vehicle-treated 3 days post-rodent nonarteritic anterior ischemic optic neuropathy (rNAION). Iba1-positive cells are relatively ameboid (globular) in appearance and increased in number. **C**: Minocycline-treated, 3 days post-rNAION. Microglia are larger than in naïve eyes but ramified. **D**: Spectral domain-optical coherence tomography (SD-OCT) images of naïve and 30 days minocycline treatment rNAION eyes. Upper panels: preinduction. The ON and the retina are labeled in the en face view shown in the left panels, while the retinal layers are shown in the cross-sectional view shown in the right panels. There is an expansion of the space between the outer nuclear layers on either side of the nerve in the same (minocycline treated) eye 2 days post-rNAION induction, when compared to the upper (uninduced) panel). **E** and **F**: ON sections 30 days post-induction. **E**: Vehicle treated. Iba1-positive cells are globoid (reactive) in appearance (arrowheads). **F**: Minocycline treated. Iba1-positive microglia are abundant and large but ramified. **E** and **F** insets: SMI 312–positive reactivity in a low power view of the entire ON cross section of the vehicle- and minocycline-treated nerves reveal a similar pattern of axonal loss. **G**–**I**: Nox2 expression in the anterior ON. **G**: Naïve animal. Little Nox2 expression is detectable. **H**: rNAION-induced, vehicle-treated nerve. Strong Nox2 expression is apparent. **I**: rNAION-induced, minocycline-treated nerve. Nox2 expression is detectable but reduced in the anterior ON. Scale bars in **A**, **B**, **C**, **E**, **F**, **G**: 50 µm. Scale bar in **D**: 200 µm. **J**: Densitometric analysis of Iba-1 signal strength shows statistically significantly increased Iba-1 signal when compared between naïve and vehicle-treated animals (1.50±0.15 standard error of the mean (SEM) versus 7.08±0.54 SEM, six animals per group), as well between naïve and minocycline-treated (6.72±0.97 SEM, six animals per group) animals (asterisks indicate statistical significance); the difference in Iba-1 staining when vehicle- versus minocycline-treated animals are compared is not statistically significant (ANOVA; f-ratio = 0.11571, p=0.74154). **K**: Densitometric analysis comparing naïve (white bar) 11.5±1.20 SEM, vehicle-treated (black bar) 17.07±1.50 SEM, and minocycline-treated (hatched bar) 10.06±0.61 SEM (ANOVA; f-ratio = 10.51066. p=0.014213; 6.72±0.97 SEM, six animals per group) animals (asterisks indicate statistical significance). **L**: rNAION upregulation of free radicals and their downregulation by minocycline demonstrated by the MitoSOX Red reaction: naïve (white bar) 5.6±3.4 SEM, vehicle-treated (black bar) 87.60±20.34 SEM, and minocycline-treated (hatched bar) 27.0±19.9 SEM (ANOVA; f-ratio = 9.05275, p=0.023738). Asterisks indicate statistical significance.

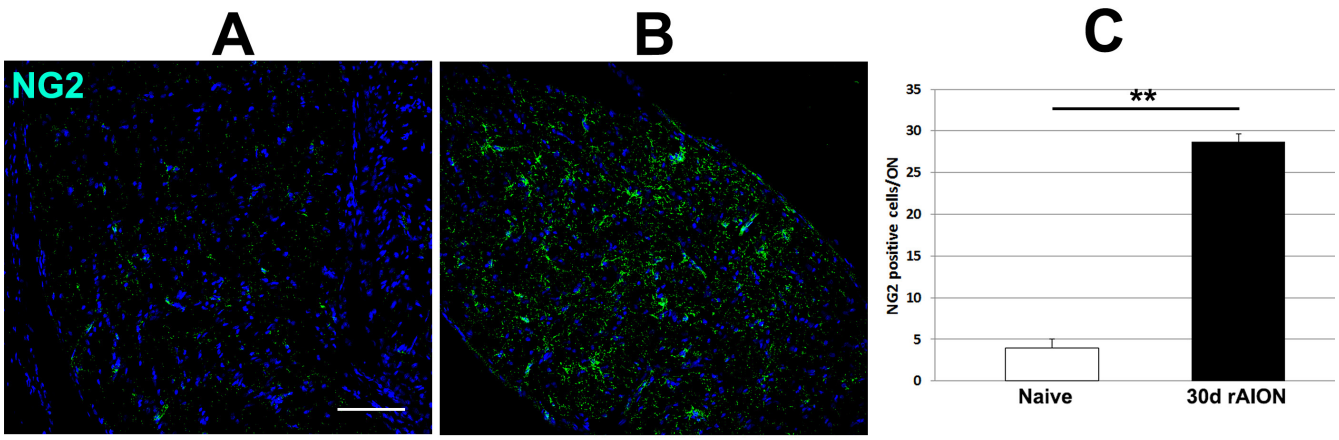

Figure 5. Changes in NG2-positive/OPCs in the anterior ON 30 day post-rNAION. **A**, **B**: Optic nerve (ON) cross sections from **A**) naïve and **B**) rodent nonarteritic anterior ischemic optic neuropathy (rNAION)-induced. There is a considerable increase in the number of oligodendrocyte progenitor cells (OPCs) present in the ON following ON ischemia. **C**: Quantification of NG2-positive/OPC increase 30 days post-rNAION. There is a 7.1-fold increase in the number of NG2-positive cells present in the rNAION-induced nerve (28.7±2.70 v. 4.0±1.9 (SEM) cells/field of view (FOV; n = 6 animals); ANOVA; f-ratio = 55.09054, p=0.000023.

As the TEM data support our previous report that post-rNAION-ON demyelination is present in the anterior ON [28] we also sought to determine whether demyelination affects the whole ON or just the anterior portion. CAPs were recorded from naïve and 30 days post-rNAION ONs 2 mm posterior to the globes, obtained from vehicle-treated animals. This preparation eliminated the primary ischemic lesion. Naïve ONs generated robust CAPs with the predicted a, b, and c waves, corresponding to large, medium, and small fibers, as previously demonstrated [28]. However, while rNAION-induced nerves showed reductions in amplitude, no apparent differences were seen in the peak conduction velocities comparing posterior portions of vehicle-treated nerves. This suggests that post-ON stroke demyelination primarily affects the anterior ON region.

rNAION generates considerable ON inflammation (see Figure 3), and previous reports revealed that early inflammation is initially cytokine based, with cellular invasion developing later [3,10]. We evaluated whether minocycline treatment induces changes in early cytokine release. Anterior ON tissue was pooled from the rNAION-induced and contralateral eyes of minocycline- and vehicle-treated rats. We isolated soluble proteins present in these tissues and analyzed them for cytokines and their relative concentrations (see the Methods section). Results from induced nerves were directly compared to extracts from the contralateral nerves that were treated in a similar fashion with either vehicle or minocycline. The results shown are mean results from pooled samples (n = 5 ONs/group); thus, there are no standard deviations. Sample values which were outside the reliable quantitative range were excluded from the analysis.

We identified several inflammatory cytokines that were expressed at either high (100–1,000 pg/ml) or low (1–100 pg/ml) concentrations (graphs, Figure 6A). High-expressing cytokines included IFNγ, MCP-1, and CX3CL1; low expressors included G-CSF, IL-4,-13, and -18, and TNF-α. M1- and M2-associated cytokines were upregulated following rNAION, compared with the contralateral eyes. Interestingly, minocycline reduced all cytokine expression in rNAION-induced tissue (compare responses of G-CSF, IL-4, and IL-13), rather than selectively reducing M1-associated cytokines alone.

Neuroprotection is the ultimate test of a drug's efficacy for post-rNAION treatment. We assessed the long-term minocycline effect on preserving RGCs. These results are shown in Figure 6. Naïve eyes show a regular pattern of RGCs across the retinal surface (Figure 6B), and individual Brn3a-positive RGCs are easily identifiable at high magnification (inset, Figure 6B). In comparison, the pattern of Brn3a-positive RGCs in flat mounted retinas from either vehicle- or minocycline-treated eyes 30 days post-induction revealed similar regional patterns of loss (compare Figure 6C,D and insets). Stereology of 17 rNAION-induced, minocycline-treated eyes was compared with that of 15 rNAION-induced, vehicle-treated eyes. Fellow eyes were used as contralateral controls (naïve; see the Methods section). Naïve eyes revealed a ratio of 1437±128.4 RGCs/mm^2 (±SEM; Figure 6E, white bar), while vehicle-treated eyes showed a ratio of 893.1±118.2/mm^2

(Figure 6E, black bar). Minocycline-treated eyes revealed a slight increase in the mean number of RGCs compared with vehicle (920.7±84.50; Figure 6E, hatched bar), but this increase was not statistically significant (ANOVA; f-ratio = 2.63798, p=0.09). Thus, minocycline does not statistically significantly protect RGCs in a long-term (30 days) format, when drug administration is begun immediately after onset of the ischemic event.

DISCUSSION

No effective treatments for NAION currently exist. Minocycline was recently proposed to have potential use in this disorder, based on a preliminary report (abstract) where investigators began administration 3 days before the stroke induction [23]. However, this approach is not a clinically relevant dosing strategy, because patients present after disease onset. As patients at highest risk for NAION (individuals who have had a previous episode in one eye) may develop NAION in the opposite eye years after the first event, continuous high dose minocycline, with its potential side effects, is not possible. Thus, we evaluated a more clinically relevant paradigm: minocycline's neuroprotective potential for post-ON ischemic treatment.

Following anterior ON ischemia, there is post-ischemic demyelination and gliosis (demonstrated in Figure 1), in addition to axonal loss. Similar to other CNS insults, we also saw an increase in NG2-positive OPCs. However, the simple presence of OPCs also does not prove functional remyelination, as multiple studies have revealed that most post-damage OPCs are not associated with maturation into oligodendrocytes [36,37].

Post-NAION, residual ON function improves in 40% of patients. This suggests that mechanisms other than primary RGC death may play important roles in preserving remaining vision. Because many axons may remain viable even after demyelination, we wanted to evaluate the direct effects of in vivo ischemia on oligodendrocytes distal to the primary insult. Previous studies identified early (within 3 days) signs of oligodendrocyte stress along the entire ON [30]. In the current study, we find that unlike RGCs, ON oligodendrocytes do not die rapidly after rNAION induction. Rather, oligodendrocyte loss is prolonged, with oligodendrocyte loss beginning much later than RGCs. The majority of

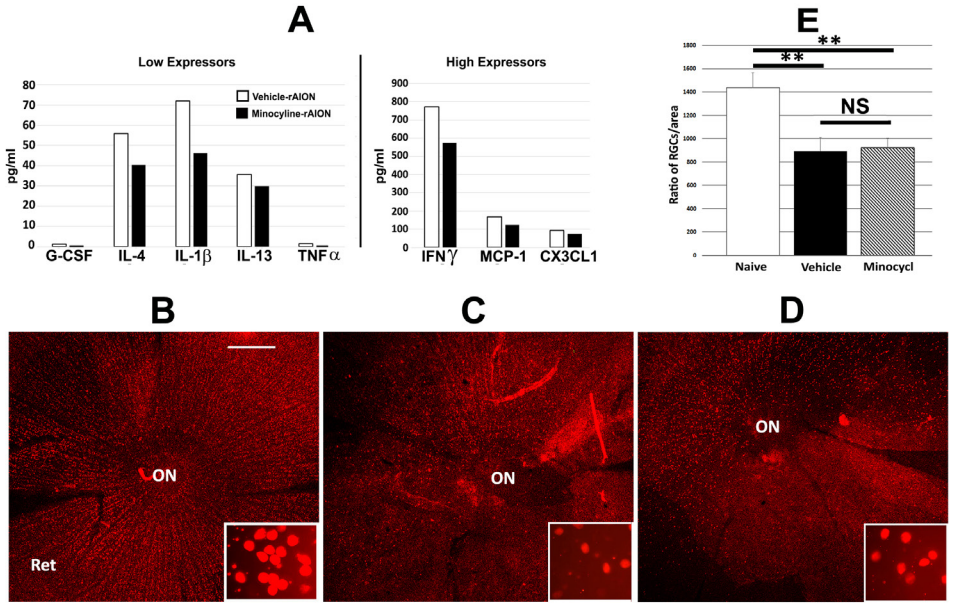

Figure 6. Minocycline treatment does not neuroprotect RGCs following rNAION induction and cytokine analysis. **A**: Cytokine analyses of vehicle- and minocycline-treated anterior optic nerves (ONs) 3 days post-rNAION induction. Five anterior ON segments were pooled from each condition and compared to the uninduced contralateral eye (vehicle-treated rodent nonarteritic anterior ischemic optic neuropathy (rNAION) induced against contralateral naïve: White bars. Minocycline-treated rNAION induced against contralateral eye: Black bars). Assays shown are all individual analyses with expression statistically significantly above baseline. Low-level (expression (1–10 pg/ml; graph shown on the left) and high-level (100–900 pg/ml; graph shown on the right) values were obtained. Cytokine expression rose after rNAION induction compared with uninduced nerves, for M1-associated cytokines (TNF-α, IL-1β, and IFNγ) and M2-associated cyto- and chemokines (G-CSF, IL-4, and IL-13). **B**–**D**: Representative images of Brn3a stained retinal ganglion cells are shown. Whole mount retinas from **B**: naïve, **C**: 30 days post-rNAION vehicle, and **D**: 30 days post-rNAION minocycline-treated retinas. Panels show global retinal ganglion cell (RGC) distribution using 4X magnification and direct RGC identification using 60X magnification inserts. **E**: Stereological analysis of RGC counts per square of retina for naïve (white bar) and vehicle- (black bar) and minocycline-treated (hatched bar) retinas 30 day post-rNAION induction. There is a slight difference in residual RGC numbers when vehicle- and minocycline-treated rNAION-induced eyes are compared, but this is not statistically significant (ANOVA; f-ratio = 2.63798, p=0.09).

oligodendrocyte death begins 21 days post-insult, peaking at about 30 days post-induction, with persistent TUNEL-positive cells apparent even at 40 days post-induction, and this does not exclude other cell species. This suggests that multiple factors may impact later oligodendrocyte death, and there may be a longer window of treatment opportunity for NAION, focusing on multiple factors impacting glial function, than previously recognized.

It is now recognized that, following onset, NAION and its models are strongly associated with inflammatory processes [2,3]. The present study identified several key inflammatory features. Initially, a dense macrophage infiltration occurs by 3 days post-induction (compare Figure 3A,B), comprised of invading extrinsic macrophages and migrating microglia. This is consistent with results previously published in other studies [3]. However, even 30 days post-induction, the anterior ON still showed considerable inflammatory cellular infiltrate, while there is prolonged microglial activation in the distal nerve. As closure of the blood–brain barrier largely occurs by the end of the first week in rNAION [30], many of the inflammatory cells in the anterior ON present later in the disease course likely represent microglia. What are the inflammatory factors regulating degeneration and recovery in this region?

It is known that early cytokine induction helps regulate and direct the form of inflammatory response [21,38,39]. Cytokine induction occurs before cellular infiltration. We previously demonstrated upregulation of TNF-α and IL-1β 1 day post-rNAION ischemia [10]. In the present study, we found strong upregulation of IFNγ, MCP-1, and CX3CL1 by 3 days post-infarct. IFNγ is related to M1 extrinsic macrophage induction, all of which direct an M1 (classical neurodegenerative) response. IL-18, another M1-associated cytokine, is also upregulated. However, IL-4 and IL-13 are also upregulated, and these cytokines are associated with the M2 (alternative activation-neuroprotective) inflammatory response. Interestingly, although TNF-α is typically associated with neurodegenerative inflammation [40,41], the relative upregulation of TNF-α expression at 1 day and 3 days is much less in the rNAION model than that seen in other models of CNS damage.

While we initially attempted to analyze ON-related patterns of M1 and M2 microglial expression, it quickly became apparent that this expression paradigm is not consistent with the cellular inflammatory changes occurring after rNAION induction, supporting recent reports that microglia do not express these patterns [13,14]. Although the exact mechanism(s) of microglial activation are still elusive, a growing body of evidence suggests that upregulation of superoxide and other reactive oxygen and nitrogen species is associated with cellular damage [18]. Nox2 upregulation has been identified as a major source of oxidative radicals and has been identified as a necessary step for glial cell activation after CNS injury [42,43]. Nox2 was even upregulated 30 days after rNAION was induced. Nox2 upregulation was also associated with increased numbers of free radicals by the MitoSOX Red reaction, which at these concentrations does not discriminate between superoxide radicals produced in mitochondria and other cellular compartments.

Because minocycline has been previously suggested to selectively suppress M1 activity, as well as exerting RGC neuroprotection in the rNAION model, we critically evaluated minocycline's effects on post-infarct ON inflammation. Minocycline administration did not reduce early rNAION-induced retinal nerve fiber layer (RNFL) and ON edema, compared with vehicle treatment, with SD-OCT. Interestingly, minocycline induced subtle morphological effects on ON-Iba-1-positive inflammatory cells by 3 days post-induction, with increased size and prominence, distal to the anterior lesion. Thirty days post-induction, microglia in minocycline-treated animals exhibited a more ramified appearance, a feature typically associated with quiescence (compare Figure 4E (vehicle) with Figure 4F (minocycline treated)). However, there were no obvious differences in the degree of axonal loss analyzed either with SMI 312 reactivity or ultrastructurally. Minocycline reduced ON-Nox2 immunohistochemical reactivity, compared with ONs from vehicle-treated animals (compare Figure 4I with Figure 4H). Thus, systemic high dose minocycline administration exerts significant changes in inflammatory cell responses post-induction, but despite apparent downregulation of Nox2 expression and free radical production assessed with MitoSOX Red, it did not improve axonal preservation in the ON.

A previous report suggested that high dose minocycline selectively suppressed M1-type cytokine responses without reducing M2 cytokine expression in the CNS [18]. Multiplex cytokine analysis revealed that in the ON, there is an equivalent reduction in M1- and M2-type cytokines. Minocycline reduced M2- (G-CSF, IL-4, and IL-13) and M1-associated (TNF-α, IFNγ, and IL-18) cytokines in a similar fashion. The previous study used real-time quantitative PCR (rq-PCR)-based assays of cytokine mRNA levels, which can be subject to post-transcriptional regulation. Because of this potential drawback, we used a protein-based cytokine assay and pooled samples.

One crucial test for clinical minocycline-rNAION treatment is, of course, RGC neuroprotection. By this standard, high dose minocycline given immediately after rNAION

induction and for 4 weeks thereafter failed to significantly improve post-stroke RGC numbers, although there was a slight trend. This is particularly interesting in view of the partial suppression of activated macrophage morphological changes and the visible suppression of Nox2 and associated free radical formation, when minocycline is given after induction. It is apparent from the present study that despite minocycline-associated changes in morphological characteristics (to a more ramified appearance), reduced Nox2 expression, reduced free radical production, and decreased overall cytokine expression compared to vehicle, these changes do not necessarily reflect neuroprotective status. This suggests at least three possibilities: 1) Minocycline's level of inflammatory suppression may be insufficient for effective neuroprotection. 2) The nonselective inflammatory downregulation exerted by minocycline in the rNAION model system may also effectively inhibit neuroprotective inflammatory responses. 3) A depressed neuroinflammatory environment needs to be achieved before neural insult. In the last case, pretreatment is required to achieve RGC neuroprotection, as noted in other models of RGC degeneration, and is not appropriate for random ischemic events. It also remains an open question as to which specific inflammatory factors are involved in regulating the later stages of degeneration and regeneration post-injury. Experimental approaches using stronger global suppression in the affected region and selective differential immunomodulation may enable us to discern which of these hypotheses are correct, potentially enabling identification of more effective immunomodulatory strategies for improving post-NAION treatment.

ACKNOWLEDGMENTS

This study was supported by NIH grant R01EY015304 and a Donner Foundation grant to SLB. The authors thank Dr. Clark Nelson and Ms. Sara Francomacaro for assistance in inflammatory marker analyses and Ms. Julie Proctor for providing slides of TBI model.

REFERENCES

1. Miller NR, Arnold AC. Current concepts in the diagnosis, pathogenesis and management of nonarteritic anterior ischaemic optic neuropathy. Eye (Lond) 2015; 29:65-79. [PMID: 24993324].

2. Salgado C, Vilson F, Miller NR, Bernstein SL. Cellular inflammation in nonarteritic anterior ischemic optic neuropathy and its primate model. Arch Ophthalmol 2011; 129:1583-191. [PMID: 22159678].

3. Zhang C, Guo Y, Miller NR, Bernstein SL. Optic nerve infarction and post-ischemic inflammation in the rodent model of anterior ischemic optic neuropathy (rAION). Brain Res 2009; 1264:67-75. [PMID: 19401181].

4. Bernstein SL, Guo Y, Kelman SE, Flower RW, Johnson MA. Functional and cellular responses in a novel rodent model of anterior ischemic optic neuropathy. Invest Ophthalmol Vis Sci 2003; 44:4153-62. [PMID: 14507856].

5. Slater BJ, Mehrabian Z, Guo Y, Hunter A, Bernstein SL. Rodent Anterior Ischemic Optic Neuropathy (rAION) Induces Regional Retinal Ganglion Cell Apoptosis with a Unique Temporal Pattern. Invest Ophthalmol Vis Sci 2008; 49:3671-6. [PMID: 18660428].

6. Batchelor PE, Tan S, Wills TE, Porritt MJ, Howells DW. Comparison of inflammation in the brain and spinal cord following mechanical injury. J Neurotrauma 2008; 25:1217-25. [PMID: 18986223].

7. Gomes-Leal W, Corkill DJ, Picanco-Diniz CW. Systematic analysis of axonal damage and inflammatory response in different white matter tracts of acutely injured rat spinal cord. Brain Res 2005; 1066:57-70. [PMID: 16325784].

8. Minami M, Katayama T, Satoh M. Brain cytokines and chemokines: roles in ischemic injury and pain. J Pharmacol Sci 2006; 100:461-70. [PMID: 16682788].

9. Avraham BC, Dotan G, Hasanreisoglu M, Kramer M, Monselise Y, Cohen Y, Weinberger D, Goldenberg-Cohen N. Increased plasma and optic nerve levels of IL-6, TNF-alpha, and MIP-2 following induction of ischemic optic neuropathy in mice. Curr Eye Res 2008; 33:395-401. [PMID: 18398714].

10. Nicholson JD, Puche AC, Guo Y, Weinreich D, Slater BJ, Bernstein SL. PGJ2 Provides Prolonged CNS Stroke Protection by Reducing White Matter Edema. PLoS One 2012; 7:e50021-[PMID: 23284631].

11. Carmichael ST. Gene expression changes after focal stroke, traumatic brain and spinal cord injuries. Curr Opin Neurol 2003; 16:699-704. [PMID: 14624079].

12. Cherry JD, Olschowka JA, O'Banion MK. Neuroinflammation and M2 microglia: the good, the bad, and the inflamed. J Neuroinflammation 2014; 11:1-32. [PMID: 24889886].

13. Morganti JM, Riparip LK, Rosi S. Call Off the Dog(ma): M1/M2 Polarization Is Concurrent following Traumatic Brain Injury. PLoS One 2016; 11:e0148001-[PMID: 26808663].

14. Ransohoff RM. A polarizing question: do M1 and M2 microglia exist? Nat Neurosci 2016; 19:987-91. [PMID: 27459405].

15. Carty ML, Wixey JA, Colditz PB, Buller KM. Post-insult minocycline treatment attenuates hypoxia-ischemia-induced neuroinflammation and white matter injury in the neonatal rat: a comparison of two different dose regimens. Int J Dev Neurosci 2008; 26:477-85. [PMID: 18387771].

16. Cho KO, La HO, Cho YJ, Sung KW, Kim SY. Minocycline attenuates white matter damage in a rat model of chronic cerebral hypoperfusion. J Neurosci Res 2006; 2006:285-91. [PMID: 16385583].

17. Fan R, Xu F, Previti ML, Davis J, Grande AM, Robinson JK, Van Nostrand WE. Minocycline reduces microglial

activation and improves behavioral deficits in a transgenic model of cerebral microvascular amyloid. J Neurosci 2007; 27:3057-63. [PMID: 17376966].

18. Kobayashi K, Imagama S, Ohgomori T, Hirano K, Uchimura K, Sakamoto K, Hirakawa A, Takeuchi H, Suzumura A, Ishiguro N, Kadomatsu K. Minocycline selectively inhibits M1 polarization of microglia. Cell Death Dis 2013; 4:e525-[PMID: 23470532].

19. Scholz R, Sobotka M, Carmoy A, Stempfl T, Moehle C, Langmann T. Minocycline counter-regulates proinflammatory microglia responses in the retina and protects from degeneration. J Neuroinflammation 2015; 12:209-24. [PMID: 26576678].

20. Cobb CA, Cole MP. Oxidative and nitrative stress in neurodegeneration. Neurobiol Dis 2015; 84:4-21. [PMID: 26024962].

21. Correale J. The role of microglial activation in disease progression. Mult Scler 2014; 20:1288-95. [PMID: 24812046].

22. Aras M, Altas M, Motor S, Dokuyucu R, Yilmaz A, Ozgiray E, Seraslan Y, Yilmaz N. Protective effects of minocycline on experimental spinal cord injury in rats. Injury 2015; 46:1471-4. [PMID: 26052053].

23. Fel A, Froger NG, Simonutti M, Bernstein NR, Bodaghi B, Lehoang P. Minocycline as a neuroprotective agent in a rodent model of NAION. Invest Ophthalmol Vis Sci 2014; 55:5736-.

24. Bosco A, Inman DM, Steele MR, Wu G, Soto I, Marsh-Armstrong N, Hubbard WC, Calkins DJ, Horner PJ, Vetter ML. Reduced retina microglial activation and improved optic nerve integrity with minocycline treatment in the DBA/2J mouse model of glaucoma. Invest Ophthalmol Vis Sci 2008; 49:1437-46. [PMID: 18385061].

25. Levkovitch-Verbin H, Kalev-Landoy M, Habot-Wilner Z, Melamed S. Minocycline delays death of retinal ganglion cells in experimental glaucoma and after optic nerve transection. Arch Ophthalmol 2006; 124:520-6. [PMID: 16606878].

26. Nicholson JD, Guo Y, Bernstein SL. SUR1-Associated Mechanisms Are Not Involved in Ischemic Optic Neuropathy 1 Day Post-Injury. PLoS One 2016; 11:e0148855-[PMID: 27560494].

27. Schmitz C, Hof PR. Design-based stereology in neuroscience. Neuroscience 2005; 130:813-31. [PMID: 15652981].

28. Slater BJ, Vilson F, Guo Y, Weinreich D, Hwang S, Bernstein SL. Optic nerve Inflammation and demyelination in a rodent model of nonarteritic anterior ischemic optic neuropathy. Invest Ophthalmol Vis Sci 2013; 54:7952-61. [PMID: 24065807].

29. Sofroniew MV, Vinters HV. Astrocytes: Biology and Pathology. Acta Neuropathol 2010; 119:7-35. [PMID: 20012068].

30. Goldenberg-Cohen N, Guo Y, Margolis FL, Miller NR, Cohen Y, Bernstein SL. Oligodendrocyte Dysfunction Following Induction of Experimental Anterior Optic Nerve Ischemia. Invest Ophthalmol Vis Sci 2005; 46:2716-25. [PMID: 16043843].

31. Dratviman-Storobinsky O, Hasanreisoglu M, Offen D, Barhum Y, Weinberger D, Goldenberg-Cohen N. Progressive damage along the optic nerve following induction of crush injury or rodent anterior ischemic optic neuropathy in transgenic mice. Mol Vis 2008; 14:2171-9. [PMID: 19052651].

32. Bhat RV, Axt KJ, Fosnaugh JS, Smith KJ, Johnson KA, Hill DE, Kinzler KW, Baraban JM. Expression of the APC tumor suppressor protein in oligodendroglia. Glia 1996; 17:169-74. [PMID: 8776583].

33. Loane DJ, Kumar A, Stoica BA, Cabatbat R, Faden AI. Progressive neurodegeneration after experimental brain trauma: association with chronic microglial activation. J Neuropathol Exp Neurol 2014; 73:14-29. [PMID: 24335533].

34. Taylor RA, Sansing LH. Microglial responses after ischemic stroke and intracerebral hemorrhage. Clin Dev Immunol 2013; 2013:746068-[PMID: 24223607].

35. Hackett AR, Lee JK. Understanding the NG2 Glial Scar after Spinal Cord Injury. Front Neurol 2016; 7:199-[PMID: 27895617].

36. Foote AK, Blakemore WF. Inflammation stimulates remyelination in areas of chronic demyelination. Brain 2005; 128:528-39. [PMID: 15699059].

37. Franklin RJ. ffrench-Constant C. Remyelination in the CNS: from biology to therapy. Nat Rev Neurosci 2008; 9:839-55. [PMID: 18931697].

38. Anderson WD, Makadia HK, Greenhalgh AD, Schwaber JS, David S, Vadigepalli R. Computational modeling of cytokine signaling in microglia. Mol Biosyst 2015; 11:3332-46. [PMID: 26440115].

39. Corna G, Campana L, Pignatti E, Castiglioni A, Tagliafico E, Bosurgi L, Campanella A, Brunelli S, Manfredi AA, Apostoli P, Silvestri L, Camaschella C, Rovere-Querini P. Polarization dictates iron handling by inflammatory and alternatively activated macrophages. Haematologica 2010; 95:1814-22. [PMID: 20511666].

40. Sehara Y, Hayashi T, Deguchi K, Zhang H, Tsuchiya A, Yamashita T, Lukic V, Nagai M, Kamiya T, Abe K. Decreased focal inflammatory response by G-CSF may improve stroke outcome after transient middle cerebral artery occlusion in rats. J Neurosci Res 2007; 85:2167-74. [PMID: 17497673].

41. Stoll G, Jander S, Schroeter M. Detrimental and beneficial effects of injury-induced inflammation and cytokine expression in the nervous system. Adv Exp Med Biol 2002; 513:87-113. [PMID: 12575818].

42. Noubade R, Wong K, Ota N, Rutz S, Eidenschenk C, Valdez PA, Ding J, Peng I, Sebrell A, Caplazi P, DeVoss J, Soriano RH, Sai T, Lu R, Modrusan Z, Hackney J, Ouyang W. NRROS negatively regulates reactive oxygen species during host defence and autoimmunity. Nature 2014; 509:235-9. [PMID: 24739962].

43. Loane DJ, Byrnes KR. Role of microglia in neurotrauma. Neurotherapeutics 2010; 7:366-77. [PMID: 20880501].

Articles are provided courtesy of Emory University and the Zhongshan Ophthalmic Center, Sun Yat-sen University, P.R. China. The print version of this article was created on 17 December 2017. This reflects all typographical corrections and errata to the article through that date. Details of any changes may be found in the online version of the article.